Temporal Development and Properties of an Overdense Plasma Produced by High Power Microwaves in a Coaxial Discharge Device

B. Kampmann

Institut für Experimentalphysik II, Ruhr-Universität Bochum, D-4630 Bochum 1

Z. Naturforsch. **34 a**, 414–422 (1979); received August 8, 1978

A coaxial plasma-waveguide-system exhibits strong absorption near its dipole resonance. Due to the plasmaguide-mode overdense plasmas can be generated in this device. Ionization dynamics and properties of this discharge are investigated by means of different diagnostic methods; the results are compared with analytical calculations of the dispersion relation in the plasma-waveguide-system. In this way the occurrence of nonlinear absorption mechanisms in presence of strong microwave fields is examined.

1. Introduction

Several authors have reported discharge devices where a plasma is generated by microwaves inside a waveguide. Beust and Ford [1] discussed "arcing" in waveguides at atmospheric pressure. Bethke and Ruess [2] investigated plasma shield propagation towards the microwave source in a waveguide, particularly looking for mechanisms of propagation; they found the generated electron density near the cut-off density n_c. Batenin et al. [3] describe a coaxial discharge with a discharge tube placed inside a rectangular waveguide, where ionization fronts move towards the microwave source. (This type of ionization front will be called "backward ionization front" furtheron.)

A homogeneous plasma column situated in a rf-electric field shows a dipole resonance at $\omega = \omega_p/\sqrt{2}$, ω_p denoting the plasma frequency, resp. at $n = 2\,n_c$, n_c denoting the cut-off density (Tonks [4, 5]). The absorption caused by the dipole resonance of the plasma column has been used by Beerwald and Kampmann [6] to generate overdense plasmas ($n \gg n_c$) in a coaxial discharge device. The overdense plasma column is created as a "forward ionization front" that expands in the direction of propagation of the microwaves; it may be kept in a steady state in contrast to the backward ionization front which only generates a transient plasma sheath.

Temporal development and properties of a pulsed coaxial discharge at high microwave power level are described in this work ($f = 9.4$ GHz; $P_{mw} \lesssim 180$ kW). Measurement of absorption and spectroscopical determination of electron density allow comparisons with analytical calculations [7], so that it is possible to look at the occurrence of nonlinear absorption mechanisms.

A steady-state discharge at medium microwave power level that shows electron densities near the dipole resonance – and therefore allows conclusions concerning relative electron density profiles – is described in [8].

Reprint requests to Dr. B. Kampmann. — Please order a reprint rather than making your own copy.

0340-4811 / 79 / 0400-0414 $ 01.00/0

2. Experimental Apparatus

The experimental set up for a pulsed discharge is shown in Figure 1. A pulse magnetron 4J50 generates microwave pulses at $f = 9.4$ GHz; the pulses are fed through an isolator to a transition section that produces a H_{11}-mode in a circular waveguide. A discharge tube of quartz is placed coaxially inside the slotted waveguide. At the end of the waveguide a horn antenna radiates the microwaves to an absorber.

The pulse length may be varied continuously since the magnetron is driven by a hard tube pulser (e. g. [9]); the maximum duration of the pulse is 6 μs. The maximum microwave power at which no sparks are generated inside the device was $P_{mw} \lesssim 180$ kW at 2 μs pulse duration length.

The radius of the circular waveguide is $a = 12.5$ mm; the outer radius of the quartz tube is $r_q = 5.5$ mm and its inner radius $r_p = 4.5$ mm. The parameters for calculation are chosen according to [7]:

$$\frac{\omega a}{c} = 2.46\,, \quad \frac{r_p}{a} = 0.36\,,$$

$$\frac{r_q}{a} = 0.44\,, \quad \varepsilon_q = 3.75\,,$$

where ε_q is the dielectric constant of quartz.

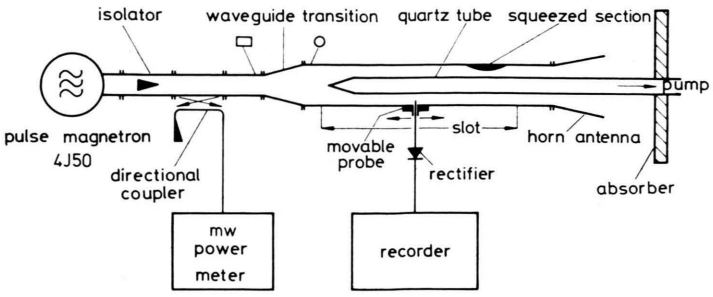

Fig. 1. Experimental apparatus.

3. Ionization Dynamics in a Coaxial Microwave Discharge

The temporal development of the discharge has been registrated by means of a streak camera; the discharge is viewed through the slot of the waveguide. In order to get a sufficiently reproduceable discharge, the waveguide has a squeezed section in case of the measurements reported in Section 3 (cf. [6]); the electric field strength is enhanced in the squeezed section so that the breakdown reproduceably occurs in this region of the waveguide. – Between 30 and 60 discharges were superimposed in order to get sufficient intensity for the streak pictures considered below.

Figure 2 shows the ionization dynamics in neon for two different neutral gas pressures. In case of Fig. 2 a breakdown occurs – about 0.5 μs earlier than in Fig. 2 b – at the squeezed section of the slotted line and a backward ionization front moves continuously towards the microwave generator. After the front end of the discharge tube is reached, a forward ionization front moves in the opposite direction. In this case the plasma is sustained by the microwave even after the ionization front has passed: the plasma continues to emit light. (Unfortunately the sensitivity of the image converter tube is somewhat reduced in the middle of the streak picture.)

This ionization dynamics may be understood as follows: when a discharge is formed at the squeezed section of the waveguide the increasing electron density leads to increasing absorption of the electromagnetic wave (this behaviour is plotted e. g.

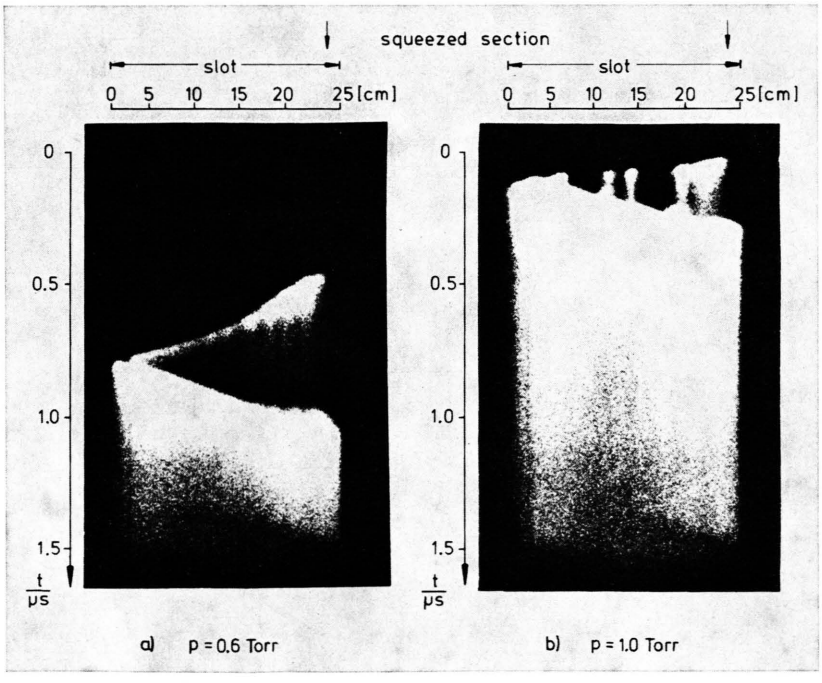

Fig. 2. Ionization dynamics in neon for two different neutral gas pressures (P_{mw} = 17 kW). (The centre of the squeezed section is marked by arrows.)

in [7], Fig. 8) and thus to an even stronger increase of electron density etc. until the cut-off region of the plasma-waveguide-system is reached and microwaves are reflected by the plasma layer. Hence, further plasma production is possible only in the part of the discharge tube between plasma and microwave source.

When an efficient transport mechanism is existing, the electron density in a volume element neighbouring the just created plasma at the side towards the microwave source will be increased, too. As before, the increased electron density leads to increasing absorption etc. In this way a backward ionization front will move to the front end of the discharge tube.

If the power level of the microwave is high enough, the electron density at the front end of the discharge tube will be increased until the region of plasma-guide-mode propagation is reached in the dispersion curve. Now increasing electron density leads to decreasing absorption of the microwave (cf. Fig. 11 or [7], Figure 8). So the microwaves may now reach and ionize regions behind the dense plasma; thus a forward ionization front propagates.

Before the breakdown occurs, there exist standing microwaves on the waveguide; they lead to enhanced ionization in the maxima of the standing waves. Therefore structures can be seen at distances of $\lambda_g/2$, where λ_g is the wavelength of microwaves in the waveguide in case no plasma is present.

As mentioned above, the backward ionization front needs a sufficiently strong transport mechanism affecting the electron density in order to produce a continuously moving plasma sheath. When the gain of electrons in a volume element due to ionization by microwaves is larger than the gain of electrons due to transport mechanisms, the backward ionization front is disrupted and continues from the volume element just considered. In case of Fig. 2 b the ionization rate has been increased by increasing neutral gas pressure until the backward ionization front was disrupted.

Transport mechanisms have been discussed in detail by Bethke and Ruess [2]; an important mechanism – beside electron diffusion – is ionization by optical radiation between 110 nm and 200 nm.

After the backward ionization front has created a plasma, this plasma only glows weakly because most of the microwave power is absorbed or reflected in the "head" of the ionization front. As the decay of the plasma generated by the backward ionization

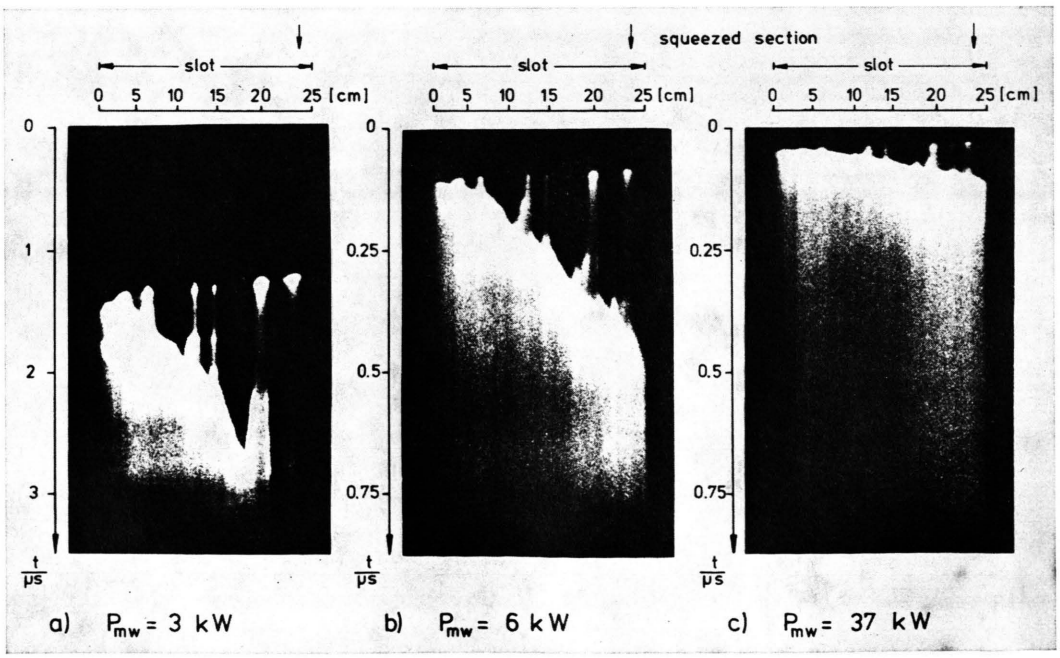

Fig. 3. The influence of microwave power on the propagation of ionization fronts in case of low collision frequency ν (Ne; $p = 6.5$ Torr).

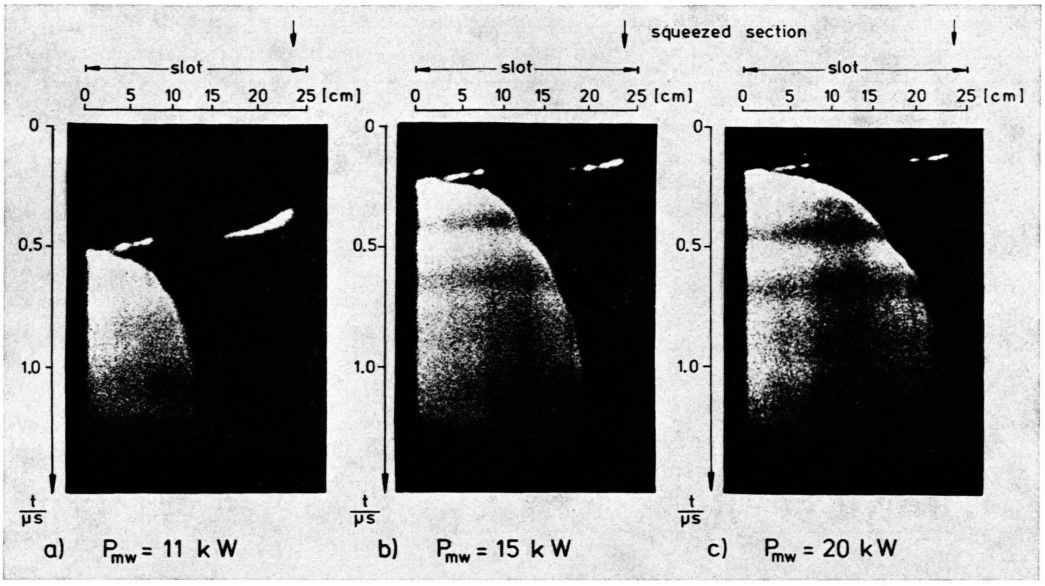

Fig. 4. The influence of microwave power on the propagation of ionization fronts in case of high collision frequency ν (H_2; $p = 1.0$ Torr).

front lasts a time long compared to the time needed by the forward ionization front to arrive at a certain volume element, the velocity of the forward ionization front is increased due to preionization by the backward ionization front. This may be seen at the end of the slotted line or at regions where the backward ionization front has been disrupted and therefore no preionization exists.

The effect of increasing microwave power level is shown in two examples: at low collision frequency and high neutral gas pressure in Ne (Fig. 3) the backward ionization front is discontinuous also for relative low microwave power levels. As the relative absorption of microwaves is small for the parameters chosen here, the velocity of the forward ionization front nearly remains constant over the length of the discharge tube in case of medium and high power level. Therefore also the ionization "spots" generated by the backward ionization front may develope to slow backward ionization fronts themselves even during the existence of the forward ionization front. In hydrogen the relative damping of microwaves is quite strong due to a high rate of collisions ν. So the velocity of the forward ionization front is decreasing more and more with decreasing microwave power along the discharge tube and a plasma column of finite length is created (Figure 4). The velocity depends on the actual microwave power level for a given position at the discharge tube: this may be seen quite well in Figs. 4 b and 4 c where – due to a small modulation of microwave amplitude – velocity and light intensity are correlated. The total length of the generated plasma column depends on the power level of the microwave pulses.

At high power levels in hydrogen and argon the discharge starts immediately as forward ionization front. The dependence of the velocity on the microwave power level is shown in Fig. 5 for hydrogen and $p = 3.0$ Torr; it may be approximated roughly by $v \sim \sqrt{P_{mw}}$ in the given range of parameters. As argued before the forward ionization front is not caused by transport processes; so its high velocity is something like a phase velocity – largely uneffected by the transport of electrons or ions.

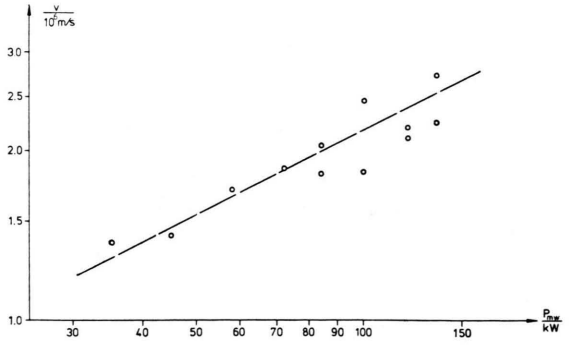

Fig. 5. The velocity of forward ionization fronts as function of microwave power (H_2; $p = 3.0$ Torr).

4. The Development of Electron Density in the Forward Ionization Front

The electron density increases very fast in the head of the forward ionization front as has been seen from the transmission of 35 GHz microwaves through the forward ionization front [10]. In less than 100 ns the cut-off density of the 35 GHz microwaves is exceeded ($n_e = 1.5 \cdot 10^{13}\,\mathrm{cm}^{-3}$).

Once the overdense plasma column is generated, electron density only increases slowly. Spectroscopic measurements of hydrogen line profiles (cf. Section 5.2) give the increase of electron density as function of time. As no optical shutter was available, the photomultiplier signal was averaged over different time intervalls and then sampled with a track & hold module. Figure 6 shows the evaluated electron densities as function of the time intervall. The electron density rises slightly as a function of time and appears to approach a limiting value. So in the following the overdense plasma column created by the forward ionization front will be investigated in the phase towards the end of the microwave pulse.

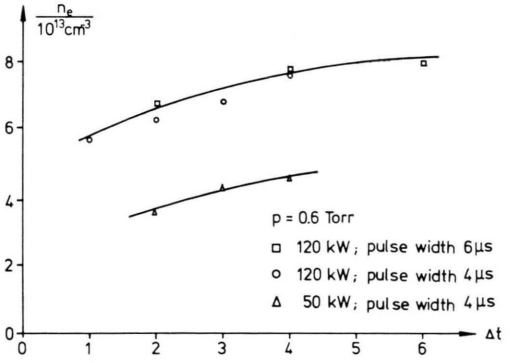

Fig. 6. Electron density of the plasma as function of the time intervall the photomultiplier signal has been integrated for.

5. Absorption of Microwaves in an Overdense Plasma Column Generated by a Forward Ionization Front

In this section the absorption of microwaves is measured and compared to analytical calculations.

5.1. Measurement of Absorption

The absorption of microwaves is calculated from the decrease of microwave power along the slotted line. Using the experimental set up of Fig. 1, the measurement is carried out as follows: the microwave signal is coupled out of the slotted waveguide by means of a capacitive probe, rectified by a microwave diode and sampled by a track & hold module. A low pass filter averages the signal over some 20 . . . 50 shots and the averaged signal is registrated as a function of probe position along the slotted line. The track & hold module is switched to "hold" shortly before the end of the microwave pulse.

The usable length of the slotted line is only about 25 cm; so several diagrams have to be combined in order to get the decrease of microwave power from high power levels to such low power levels which cause no further ionization. Figure 7 a shows the absorption of microwave power along the active discharge; it is obtained from 12 single diagrams. The spread of the measured points is mainly caused by standing waves on the slotted line due to reflection of microwaves by electron density gradients in

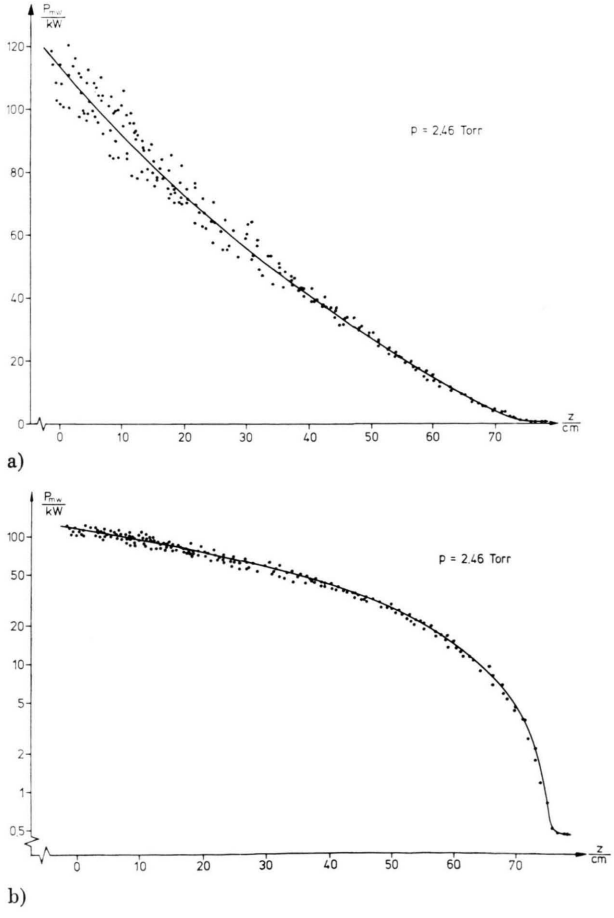

Fig. 7. Decrease of microwave power along the discharge. a) linear plot; b) logarithmic plot.

z-direction. The microwave power decreases from $P_{mw} = 120\,kW$ to about $P_{mw} = 0.5\,kW$; the decrease is by far stronger than exponential. This may be seen from Fig. 7 b in a logarithmic plot: the slope corresponds to the relative absorption of the microwave. Along the generated plasma column the relative absorption increases by a factor of 30 in this diagram. A regulating mechanism leads to a steady state equilibrium of the plasma column: for a given value of microwave power the relative absorption decreases when the electron density is raised from its equilibrium value (e. g. Fig. 11) and for that very reason absorbed power and electron production rate decrease, too; on the other hand electron losses are increased at higher electron density so that the system will return to the equilibrium value of electron density. Vice versa absorbed power and electron production rate increase with decreasing electron density while diffusion losses will decrease. Therefore a stationary equilibrium will be established versus the end of the microwave pulse in any section of the plasma column. The equilibrium state will change at a time scale where expansion of the heated neutral gas must be taken into account; this should be important in case of extremely long microwave pulses and may be neglected here.

Figure 8 gives the normalized relative absorption $-\mathrm{Im}(k\,a)$ (cf. [7]) as function of microwave power for several neutral gas pressures. The relative absorption decreases with increasing microwave power and therefore also with increasing electron density. The smallest values of $-\mathrm{Im}(k\,a)$ correspond to an absorption length of about 2 m for a decrease of microwave power by a factor $1/e$, so that numerous diagrams had to be combined due to the short length of the slotted waveguide.

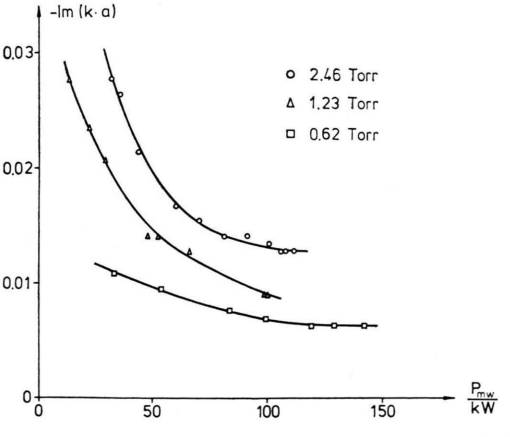

Fig. 8. The measured relative absorption $-\mathrm{Im}(k\,a)$ in the plasma-waveguide-system as function of microwave power.

For comparison with calculations the normalized collision frequencies ν/ω may be determined according to Cottingham and Buchsbaum [11] from:

$$\nu_i = 4.8 \cdot 10^9 (p/\mathrm{Torr}) \cdot \mathrm{s}^{-1}$$

as:

$$p = 0.62\,\mathrm{Torr}: \ \nu/\omega = 0.05;$$
$$p = 1.23\,\mathrm{Torr}: \ \nu/\omega = 0.1;$$
$$p = 2.46\,\mathrm{Torr}: \ \nu/\omega = 0.2.$$

5.2. *Spectroscopic Measurement of Electron Density*

The electron density of the plasma generated by the forward ionization front was estimated from hydrogen line profiles. As the line profiles were affected by Stark broadening as well as by Doppler broadening in our case, the analysis of the measured line profiles was based on unified theory calculations by Vidal et al. [12]. A method to evaluate neutral gas temperature and electron density from half width (or quarter width) of pair of lines H_β and H_δ has been given in [10]. At electron densities above $n = 10^{13}\,\mathrm{cm}^{-3}$ the resolving power of this method is quite satisfactory: the values of electron density resulting from half width and from quarter width usually differ less than 5%.

The line profiles were recorded by means of a 1 m-Czerny-Turner spectrograph (Spex Ind., 1704) and a photomultiplier (EMI 9558 QB) with a track & hold circuit. Light from a 5 cm long section of the plasma was focused on the entrance slit of the spectrograph. As this section of the plasma was located in the middle of the slotted waveguide, electron density, microwave power and relative absorption could be measured at the same position.

Figure 9 shows the increase of electron density with rising microwave power. As the intensity of H_δ decreases for high neutral gas pressure, the evaluated electron densities scatter relatively strong in case of Figure 9 c. At the maximum power level used here electron densities up to $n = 8 \cdot 10^{13}\,\mathrm{cm}^{-3}$ – respec. $n/n_c = 80$ – are generated.

In Fig. 10 electron density is plotted against the absorbed microwave power per cm length of the discharge. For a given electron density the absorbed power does not decrease with increasing neutral gas

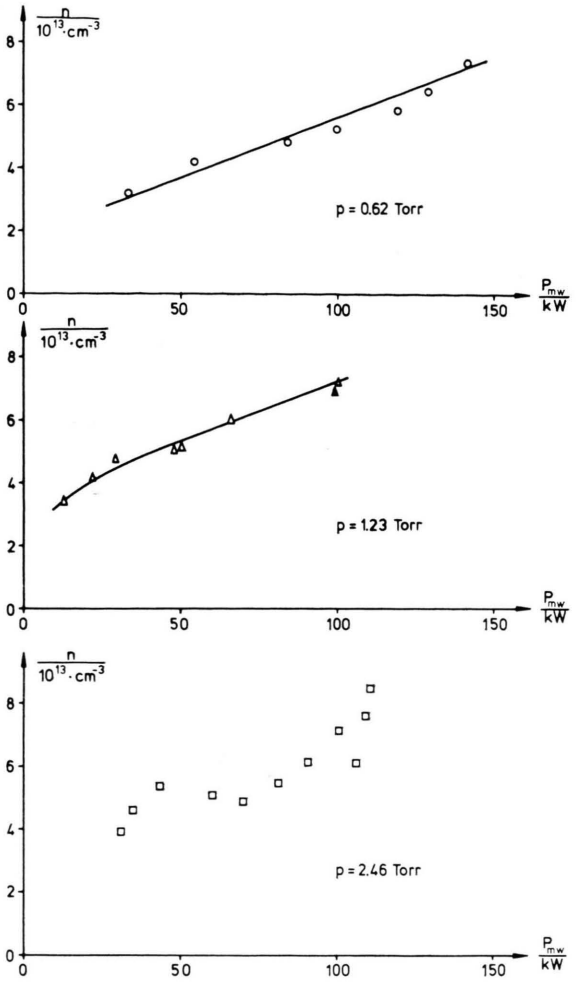

Fig. 9. Spectroscopically measured electron density as function of microwave power.

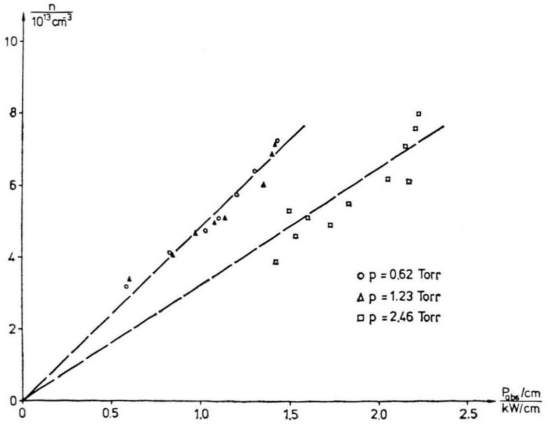

Fig. 10. Electron density as depending on absorbed microwave power per cm length of the discharge.

pressure but remains constant resp. rises. As diffusion losses of electron density decrease with increasing neutral gas pressure, the relative density profiles must be steeper in case of high pressure. For given neutral gas pressure the electron density rises almost linearly with absorbed microwave power: this leads to the conclusion that the relative electron density profile does not change considerably within the range of microwave power level considered here.

The light emitted by the discharge was investigated by looking axially into the discharge [15]. At high neutral gas pressure light is emitted from the edge of the plasma and the inner part of the plasma column remains dark. As this result was not changed by increasing microwave power or pulse duration length the decrease of light intensity in the inner part of the plasma column must be due to a decrease of electron temperature. In accordance to theory [7] this demonstrates that the microwave power is absorbed in the outer part of the plasma column. Moreover, this had to be expected due to the small skin depth of the microwave.

5.3. Discharge in Helium

For the given parameters of the experimental apparatus a microwave power level of $P_{mw} = 150\,kW$ leads to an effective electrical field strength of $E = 6\,kV/cm$. So the question rises, whether this high electrical field strength probably will be able to excite instabilities.

As the spectrum of pulse magnetrons is quite disturbed, it is not possible to detect parametric decay by means of a spectrum analyzer. Strong electric fields in plasmas, however, may be found looking to forbidden lines of Helium (e. g. Baranger, Mozer [13]): field fluctuations will cause satellites symmetric to the forbidden line at a distance corresponding to the frequency of the fluctuation. In absence of fluctuations the relative height of the forbidden line (as compared to the main line) is determined by the Holtsmark field strength and may be used to determine the electron density (e. g. Barnard et al. [14]).

By using a mixture of hydrogen and helium, the electron density could be determined from Stark broadening of hydrogen lines; the forbidden helium line near 4471.48 Å did not appear to be increased considerably.

In [15] the experimental line profile of a discharge in He ($p = 4.5$ Torr; $P_{mw} = 70$ kW) shows good agreement to a calculated line profile given in [14] where the theoretical line profile has been calculated for an electron density of $n = 3.2 \cdot 10^{14}\,cm^{-3}$. Fluctuations near the plasma frequency – probably due to parametric decay into two Langmuir waves – would cause satellites. According to Baranger and Mozer [13] one may estimate an upper limit for the amplitude of fluctuations from the amplitude of noise ($\approx 1‰$ of the main line intensity) to be about 2 kV/cm. So in helium parametric decay into Langmuir waves should not contribute considerably to the absorption of microwaves. This is in accordance to measurements in a steady-state discharge at medium microwave power level [8], where parametric decay can be found only at low power levels as the threshold for parametric decay increases with increasing electron density gradient (Perkins and Flick [16]).

5.4. *Comparison of Experimental Results to Analytical Calculations*

The real part of the wave vector was determined from the distance of maxima of standing waves on the slotted waveguide in case of a high density plasma and in case without plasma. As[7], Fig. 11 shows, the real part of $k\,a$ is a slowly varying function of electron density for $n/n_c > 50$.

The theoretical values were calculated for a homogeneous plasma column and $n/n_c = 50$; the relative collision frequency was taken to be $\nu/\omega = 0.1$, corresponding to experiment. The difference of analytical and experimental results is smaller than 1%:

without plasma: $\mathrm{Re}(k\,a)_{th} = 1.909$;
$\mathrm{Re}(k\,a)_{exp} = 1.93$;
with plasma: $\mathrm{Re}(k\,a)_{th} = 2.432$;
$\mathrm{Re}(k\,a)_{exp} = 2.42$.

Figure 11 shows the imaginary part of $k\,a$ as function of electron density for several relative density profiles and the experimental results. The experimental values of relative absorption are even lower than the absorption of a homogeneous plasma column. This discrepancy is resolved by taking into account that the spectroscopical measurement give a mean value of electron density corresponding to the light emitting part of the plasma and that the light is emitted more and more from the outer region of the plasma when neutral gas pressure increases [15]. Provided that electron density increases in the middle of the plasma column – which emits less and less light with increasing neutral gas pressure – the estimated electron densities have to be shifted to higher values to give the peak electron density of the plasma column. If the electron density is multiplied by a factor 2 or 3 one gets similar electron density profiles as in case of a steady state discharge (cf. [8]). In accordance to this consideration the greatest correction is needed in case of Fig. 11 c where the light emission is restricted most strongly to the outer part of the plasma column.

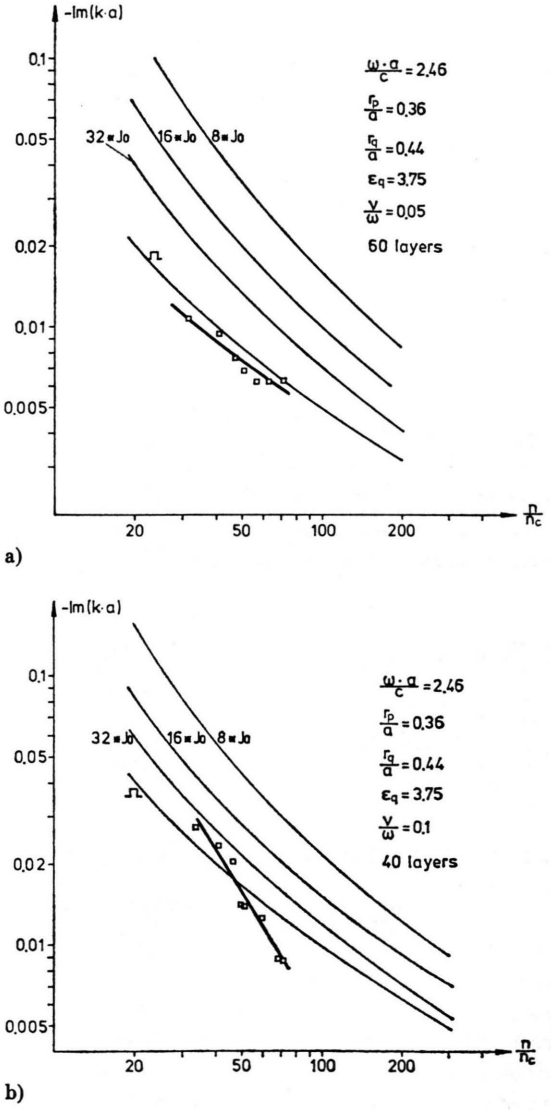

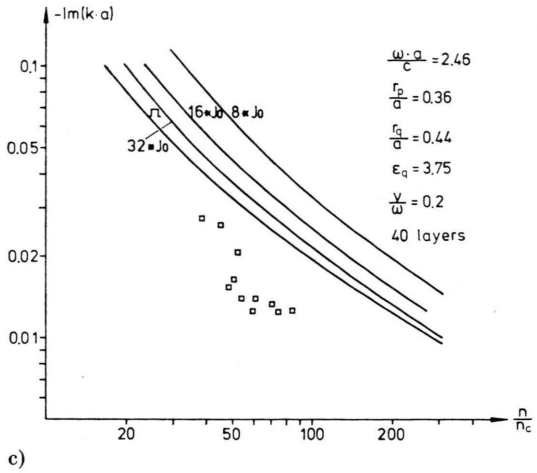

Fig. 11. Comparison of measured values of absorption $-\mathrm{Im}(k\,a)$ with calculated absorption [7]. Ω denotes a homogeneous plasma column. $m * J_0$ denotes a relative density profile $y = m * J_0(2.4\,r/r_\mathrm{p})$ that is cut at $y = 1$; this type of density profiles is chosen in order to consider the influence of different density gradients at a given maximum density. a) $p = 0.62$ Torr, b) $p = 1.23$ Torr, c) $p = 2.46$ Torr.

6. Summary

In a coaxial microwave discharge the ionization is not uniform in space but is subjected to ionization dynamics. After a backward ionization front has produced an electron density near the cut-off density n_c (waveguide-mode), the electron density rises very fast in the forward ionization front until the dipole resonance of the plasma-waveguide-system is exceeded (plasmaguide-mode). Thereafter the electron density increases slowly until an equilibrium is established. By means of high power microwave pulses ($f = 9.4$ GHz; $P_\mathrm{mw} \lesssim 180$ kW; $E \lesssim 6$ kV) one may generate high density plasmas (H_2: $n \lesssim 8 \cdot 10^{13}$ cm^{-3}; $n/n_\mathrm{c} \lesssim 80$. He: $n \lesssim 3 \cdot 10^{14}$ cm^{-3}; $n/n_\mathrm{c} \lesssim 300$) also in case of low values of ν/ω.

For collision frequencies $\nu/\omega > 0.1$ the radial distribution of light emission [15] shows – in agreement with calculations [7] – that the absorption of electromagnetic wave is restricted to the outer part of the plasma column. Since the resulting distribution of light emission is stationary, the electron density is expected to increase in the central part of the plasma column; this is suggested by the comparison of experimental results and analytical calculations of $\mathrm{Im}(k\,a)$.

Anomalous dissipation could not be observed in accordance to experiments at medium microwave power level [8] as the threshold for parametric decay increases with increasing electron density gradient.

The coaxial discharge described here constitutes a simple device to generate an electrodeless high density plasma.

Acknowledgements

These investigations have been supported by the Sonderforschungsbereich 162 "Plasmaphysik Bochum/Jülich" and partially by the DFG Schwerpunktprogramm "Fusionsorientierte Plasmaphysik". The author wishes to thank Prof. Dr. H. Schlüter and Dr. H. Beerwald for the support of the work and Mr. K. Brinkhoff for his technical assistance during the experiments and for plotting the diagrams.

[1] W. Beust and W. L. Ford, Microwave J. **4.10,** 91 (1961).
[2] G. W. Bethke and A. D. Ruess, Phys. Fluids **12,** 822 (1969).
[3] V. M. Batenin, I. I. Devyatkin, V. S. Zrodnikov, I. I. Klimovskii, and I. I. Tsemko, Teplofizika Vysokikh Temperatur **9,** 896 (1971).
[4] L. Tonks, Phys. Rev. **37,** 1458 (1931).
[5] L. Tonks, Phys. Rev. **38,** 1219 (1931).
[6] H. Beerwald and B. Kampmann, Phys. Lett. **45 A,** 95 (1973).
[7] B. Kampmann, Z. Naturforsch. **32 a,** 935 (1977).
[8] B. Kampmann, Z. Naturforsch. **34 a,** 423 (1979).
[9] G. N. Glasoe, and J. V. Lebacqz, Pulse Generators, MIT Rad. Lab. Ser., Boston Techn. Publ. Inc., Lexington, Mass. 1964.
[10] B. Kampmann, Verhandl. DPG (VI) **10,** 285 (1975).
[11] W. B. Cottingham and S. J. Buchsbaum, Phys. Rev. **130,** 1002 (1963).
[12] C. R. Vidal, J. Cooper, and E. W. Smith, Astrophys. J. Suppl. Series **25,** 37 (1973).
[13] M. Baranger and B. Mozer, Phys. Rev. **123,** 25 (1961).
[14] A. J. Barnard, J. Cooper, and E. W. Smith, J. Quant. Spect. Rad. Trans. **14,** 1025 (1974).
[15] B. Kampmann, Thesis, Ruhr-Universität Bochum 1976.
[16] W. Perkins and J. Flick, Phys. Fluids **14,** 2012 (1971).